Molecular Characterization of Atmospheric Particulate Organosulfates in Three Megacities at the Middle and Lower Reaches of the Yangtze River

X. K. Wang[1, 2, a], S. Rossignol[3, a], Y. Ma[1, 2], L. Yao[1, 2], M. Y. Wang[1, 2], J. M. Chen [1, 2], C. George[3, *], L. Wang[1, 2,*].

[1] *Shanghai Key Laboratory of Atmospheric Particle Pollution and Prevention (LAP³), Department of Environmental Science & Engineering, Fudan University, Shanghai 200433, China*

[2] *Fudan Tyndall Centre, Fudan University, Shanghai 200433, China*

[3] *Université de Lyon 1, Lyon, F-69626, France; CNRS, UMR5256, IRCELYON, Institut de Recherches Sur la Catalyse et l'Environnement de Lyon, Villeurbanne, F-69626, France*

[a] *These authors contributed equally to the work.*

* Corresponding Authors: C.G., email, Christian.George@ircelyon.univ-lyon1.fr; phone, (33)(0)437423681; fax, (33)(0)472448438. L.W., email, lin_wang@fudan.edu.cn; phone, +86-21-65643568; fax, +86-21-65642080.

Abstract. PM$_{2.5}$ filter samples have been collected in three megacities at the middle and lower reaches of the Yangtze River: Wuhan (WH), Nanjing (NJ), and Shanghai (SH). The samples were analyzed using ultra-high-performance liquid chromatography (UHPLC) coupled with Orbitrap mass spectrometry (MS), which allowed for detection of about 200 formulas of particulate organosulfates (OSs), including dozens of formulas of nitrooxy-organosulfates, with various numbers of isomers for each tentatively determined formula at each location. The number of aliphatic OS formulas represented more than 78% of the detected OSs at the three locations, while aromatic OSs were much less numerous. OSs with two to four isomers accounted for about 50% of the total OSs on average in these megacity samples, and the percentage of OSs with six and more isomers in the WH sample was more significant than those in the SH and NJ samples. Additionally, the molecular formula, average molecular weight, and degrees of oxidation and unsaturation of tentatively assigned OSs were compared. The results indicate that the OSs between NJ and SH shared higher similarity, and the characteristics of OSs in SH varied diurnally and seasonally. OSs derived from isoprene, monoterpenes, and sesquiterpenes were abundant in samples from the three megacities and could be produced through both daytime photochemistry and NO$_3$ night-time chemistry. The reaction pathways leading to isoprene-derived OSs probably varied in those locations because of the different NO$_x$ levels. In addition, a number of OSs that might be formed from polycyclic aromatic hydrocarbons were also detected, which underlies the importance of anthropogenic sources for this class of compounds.

1. Introduction

Atmospheric aerosols can scatter and absorb sunlight and provide cloud condensation nuclei. Hence, they have significant impacts on air quality and climate (Andreae and Crutzen, 1997; Hallquist et al., 2009). Aerosol particles contain a large fraction of toxic chemical substances and are harmful to human health (Magari et al., 2002; Ostro et al., 2007). Organosulfates (OSs)—i.e., sulfate esters and their derivatives formed from atmospheric heterogeneous and multiphase chemical reactions (Ma et al., 2012)—are a class of organic compounds that contribute to the total abundance of atmospheric aerosol particles (Tolocka and Turpin, 2012).

Surratt et al. (2007) were the first to identify isoprene- and α-pinene-derived OSs in ambient aerosols in the southeast US using high-performance liquid chromatography coupled with electrospray mass spectrometry. Since then, tremendous progress has been made in the understanding of the formation mechanisms of OSs. Experimental studies show that isomeric isoprene epoxydiols (IEPOX) and methacrylic acid epoxide (MAE) are formed during the oxidation of isoprene under low- and high-NO_x conditions, respectively. Subsequent acid catalyzed-reactions of IEPOX and MAE in the presence of sulfates can lead to the formation of OSs (Darer et al., 2011; Lin et al., 2012c; Lin et al., 2013; Surratt et al., 2010; Paulot et al., 2009). OSs can be formed from reactions between α-pinene and OH radicals, NO_3 radicals, and O_3 in the presence of sulfates, from β-pinene under high-NO_x conditions, from ozonolysis and photochemical reactions of other monoterpenes (α-terpinene and γ-terpinene), and from sesquiterpene (i.e., β-caryophyllene) under acidic conditions (Surratt et al., 2008; Iinuma et al., 2007a; Iinuma et al., 2007b; Chan et al., 2011). Sulfate/sulfite radical-induced oxidation reactions with unsaturated organic compounds including isoprene, methyl vinyl ketone, methacrolein, and α-pinene in the aqueous phase represent another potential formation route of OSs (Szmigielski, 2015; Rudzinski et al., 2009; Noziere et al., 2010; Schindelka et al., 2013). In addition, both reactive uptake of carbonyl compounds on sulfuric acid or sulfates (Liggio et al., 2005) and hydrolysis reactions of organonitrates can lead to formation of OSs (Darer et al., 2011; Hu et al., 2011). Very recently, OSs and sulfonates were revealed to form from

70   photo-oxidation of polycyclic aromatic hydrocarbons (PAHs) in the presence of

71   sulfate seed (Riva et al., 2015b).

72   Identification and quantification of OSs in atmospheric particulate samples have

73   been widely performed around the world (e.g., Kristensen and Glasius, 2011; Stone et

74   al., 2009; Olson et al., 2011; Zhang et al., 2012). Many studies indicate that the total

75   abundance of OSs varies from one region to another. OSs accounted for about 4% of

76   the total organic mass in ambient aerosols over the southeast Pacific Ocean (Hawkins

77   et al., 2010), whereas this contribution was estimated to be about 30% at the forested

78   site of K-puszta in Hungary during summer (Surratt et al., 2008). The abundance of a

79   given OS also shows clear variation between different sampling locations. The level

80   of four aromatic OSs was estimated to be 234.4 pg m^{-3} in atmospheric PM$_{2.5}$ in

81   Pakistan, which were much more abundant than those in California (8.9 pg m^{-3}) or

82   Nepal (3.9 pg m^{-3}) (Staudt et al., 2014).

83   In a given location, there are seasonal variations of OSs. For example, the

84   α-pinene-related nitrooxy-OSs were detected at high concentrations during the winter

85   period, followed by autumn, spring, and summer at a rural background site in Hamme,

86   Belgium (Kahnt et al., 2013). Ma et al. (2014) showed that the total mass

87   concentration of 17 OSs was the highest in summer and lowest in winter, while no

88   clear seasonal trend was observed in the mass concentration of benzyl sulfate (BS).

89   However, BS showed the highest concentration in winter and the lowest one in

90   summer in Lahore, Pakistan (Kundu et al., 2013), which underlies the role of both

91   regional constraints and meteorological conditions.

92   Recently, ultra-high-resolution mass spectrometry has been applied for tentative

93   determination of the molecular formulas of OSs in atmospheric aerosols samples.

94   Owing to the high mass resolution and mass accuracy of the ultra-high-resolution

95   mass spectrometer, the molecular formulas of analytes can be tentatively determined

96   without the authentic standards required with low-resolution mass spectrometers. Lin

97   et al. (2012a, 2012b) studied aerosols sampled at a rural location of the Pearl River

98   Delta Region in China and suggested that the arbitrary signal intensities of OSs

99   obtained from the humic-like fraction are often the strongest in the electrospray

100   ionization ultra-high resolution mass spectra, and that the degrees of oxidation of OSs

101   and nitrooxy-OSs are quite high. Using a similar approach, O'Brien et al. (2014)

102   showed that a significant portion of OSs was formed from biogenic precursors

103   through the epoxide pathway in Bakersfield, CA, USA. In addition, by using a

104   mixture of acetonitrile and toluene instead of a mixture of acetonitrile and water as the

105   working solvent for nano-DESI ionization, Tao et al. (2014) tentatively determined

106   many OSs with long aliphatic carbon chains and low degrees of oxidation and

107   unsaturation, which were presumably formed from anthropogenic precursors emitted

108   by cars in Shanghai (SH).

109   Although it has been accepted that OSs are an important component of ambient

110   particulate matter, studies on their characteristics are rather sparse in China, especially

111   in the Yangtze River region. Ma et al. (2014) identified and quantified 17 OSs in SH.

112   As mentioned, Tao et al. (2014) compared OS characteristics such as the degrees of

113   oxidation and saturation between samples from SH and Los Angeles. While SH has

114   been a relative hotspot for OS characterization, the characteristics of OSs in the

115   general Yangtze River region have yet to be elucidated. Wuhan (WH), Nanjing (NJ),

116   and SH are three megacities at the middle and lower reaches of the Yangtze River

117   with populations of over 10, 8, and 24 million, respectively (as of 2014). Tremendous

118   amounts of energy are consumed owing to the large population and rapid economic

119   development, leading to extensive emissions of anthropogenic pollutants including

120   particulate matter, volatile organic compounds (VOCs), sulfur dioxide, and nitrogen

121   oxides (Huang et al., 2011; Wang et al., 2013). At the same time, these three cities are

122   located in the subtropical zone with high emissions of biogenic VOCs (Guenther et al.,

123   1995). Hence, substantial amounts of OSs are likely to exist in WH, NJ, and SH

124   aerosol particles. In this study, OSs, including nitrogen-containing OSs, were

125   specifically searched for in WH, NJ, and SH $PM_{2.5}$ samples using

126   ultra-high-performance liquid chromatography (UHPLC) coupled to Orbitrap mass

127   spectrometry (MS). Characteristics of OSs including the molecular formula, number

128   of isomers, molecular weight, and the degrees of oxidation and unsaturation were

129   analyzed and compared. The potential precursors in the megacities are also discussed.

130

2．Material and methods

2.1 Collection of PM$_{2.5}$ samples

Eight PM$_{2.5}$ samples were collected at three locations: two in WH, two in NJ, and four in SH, as shown in Figure 1 and Table 1. Samples covering 24 h were collected in WH from January 26 to 27 (sample ID: WH winter, WHW) and from June 15 to 16, 2012 (sample ID: WH summer, WHS). The WH site was located on the rooftop of a dormitory building (30°29′N, 114°24′E) that is about 20 m above ground at ZhongNan University of Economics and Law near a commercial street. NJ samples were collected from August 29 to 30, 2012, for 12 h for each sample (samples ID: NJ summer daytime, NJSD; NJ summer nighttime, NJSN). The NJ site was located in the Chinese national meteorology observatory facility at the Nanjing University of Information Science and Technology (32°12′N，118°42′E), which is about 15 km north of the downtown area and about 2 km west of clusters of steel mills and petrochemical refinery facilities (Zheng et al., 2015).

SH samples were collected for 12 h from January 17 to 18, 2013 (sample ID: SH winter daytime, SHWD; SH winter nighttime, SHWN), and July 28 to 29, 2013 (sample ID: SH summer daytime, SHSD; SH summer nighttime, SHSN). The SH site was located on the rooftop of a teaching building at Fudan University (31°18′N，121°30′E) about 20 m above ground with surrounding residential and commercial properties and a major highway to the south of the site (Xiao et al., 2015; Ma et al., 2014). Table S1 provides a comparison of air quality and meteorological conditions between the sampling days and the seasonal average in SH.

PM$_{2.5}$ was collected on 90 mm quartz-fiber filters (Whatman Company, UK) using a middle-flow impact aerosol sampler (Qingdao Hengyuan Tech Co., Ltd., HY-100) operating at 100 Lpm. All filters were prebaked at 500°C for 5 h to remove residual organics before use. After sample collection, filters were wrapped in prebaked aluminum foil and stored at -20°C before further analysis.

2.2 Sample analysis

One-fourth of each filter was put into an amber vial with 6 mL of methanol (Optima® LC/MS, Fischer Scientific, UK) and shaken for 20 min on an orbital shaker set to 1000 rpm. The extract was then filtered through a glass syringe on a 0.2 μm PTFE membrane (13 mm, Pall Corporation, USA). These two steps were performed twice, and the extracts of each filter were recombined and blown almost to dryness under a gentle stream of nitrogen. The extracts were then reconstituted in 1 mL of a 1:1 v/v mixture of water (Optima® LC/MS, Fischer Scientific, USA) and acetonitrile (Optima® LC/MS, Fischer Scientific, USA). For the analysis, 100 μL of the final reconstituted extract was diluted by adding 100 μL of water. 5 μL of these diluted solutions (50 μL in the case of the NJSD sample) were analyzed by UHPLC (Dionex 3000, Thermo Scientific, USA) coupled to a Q-Exactive Hybrid Quadrupole-Orbitrap mass spectrometer (Thermo scientific, USA). The efficiency and the repeatability on three replicates of the extraction protocol were checked using four standards: methyl sulfate, octyl sulfate, dodecyl sulfate, and camphor sulfonic acid. The results showed that their average extraction efficiencies were 71.4, 95.0, 97.7, and 94.0%, respectively (Table S2). Analytical replicates were not considered because the final sample extract volume was quite low (200 μL), and the remaining volume after the first injection was preferentially kept in case of specific analytical doubt rather than systematically injected.

Analytes were separated using a Waters Acquity HSS T3 column (1.8 μm, 100×2.1 mm) with mobile phases consisting of (A) 0.1% formic acid in water (Optima® LC/MS, Fischer Scientific, USA) and (B) 0.1% formic acid in acetonitrile (Optima® LC/MS, Fischer Scientific, USA). The concentration of eluent B was initially kept at 1% for 2 min, then increased to 100% in 11 min, kept at 100% for 2 min, decreased to 1% in 0.1 min, and kept at 1% for 6.9 min. The Q-Exactive Hybrid Quadrupole-Orbitrap mass spectrometer was equipped with a heated electrospray ionization source. It was operated in the negative ion mode with a spray voltage of -3.0 kV, a mass resolving power of 140 000 at m/z 200, and a scanning range of 50–750 m/z. The Q-Exactive mass spectrometer was externally mass calibrated daily using a 2 mM sodium acetate solution that provides a series of negative adduct ions in

190   the range of 50–750 *m/z*.

191

192   2.3 Data processing

193   The obtained chromatograms were analyzed with Progenesis QI software (V1.0,

194   Waters Corporation) by assuming that the extracted ions in the range of 50–750 *m/z*

195   [M-H] were formed from loss of a proton from the analytes. In contrast to direct

196   infusion, the LC separation provides meaningful help in distinguishing

197   quasi-molecular ions and potential in-source formed adducts for the same

198   chromatographic retention time. A molecular formula calculator was then used to

199   mathematically assign all possible formulas for an extracted quasi-molecular ion with

200   a mass tolerance of ±2 ppm. These molecular formulas can be expressed as

201   $C_cH_hO_oN_nS_s$, where c is the number of carbon atoms in the range of 1–40, h is the

202   number of hydrogen atoms in the range of 2–80, o is the number of oxygen atoms in

203   the range of 0–40, n is the number of nitrogen atoms in the range of 0–3, and s is the

204   number of sulfur atoms in the range of 0–2. Formulas were further constrained by

205   setting H/C, O/C, N/C, S/C, and double bond equivalent to carbon number ratios

206   (DBE/C) in the ranges of 0.3–3.0, 0–3, 0–0.5, 0–0.2, and 0–1, respectively. This was

207   done to ensure that the retrieved molecular formula do exist in nature (Fuller et al.,

208   2012; Lin et al., 2012a; Lin et al., 2012b).

209   The number of ions with more than one reasonable formula within 2 ppm mass

210   tolerance accounted only for 1.5% of the total number of tentatively determined ions,

211   and the formulas with the best accuracy are listed in Table S3. The peak intensities of

212   isotopically substituted ions were constrained by their low abundance and were hence

213   not systematically checked. Compounds that satisfy these criteria and present a

214   number of oxygen atoms greater than or equal to 4s+3n ($4s+3n \leq o$) were tentatively

215   regarded as OSs or nitrooxy-OSs. However, tandem MS experiments were not

216   conducted on the S- and N-containing ions detected in these eight ambient samples.

217   Therefore, other S- and N-containing compounds, such as sulfonates or compounds

218   bearing nitro groups, may also be involved (e.g., Riva et al., 2015b; El Haddad et al.,

219   2013) due to the lack of using tandem MS experiments to provide insights into the

220   structures of these ions.

221   In this study, the abundance of an OS refers to the area of its chromatographic peak,

222   and the number of isomers for an OS is based on the number of chromatographic

223   peaks observed for given *m/z* values. Note that the obtained number of isomers may

224   vary significantly when the separation method is further optimized. Then, the

225   arbitrary abundances of all isomers for a given *m/z* value are added up. The arbitrary

226   abundance of the most abundant OS or nitrooxy-OS in each sample is defined as

227   100%, and only OSs and nitrooxy-OSs with an arbitrary abundance larger than 0.5%

228   of the most abundant one in the same sample are presented. The signal-to-noise ratios

229   of the least abundant OSs in each sample are greater than 10 with a noise level of ca.

230   1×10^4 arbitrary units. Note that the arbitrary abundance of a given OS does not

231   directly reflect its concentration compared to others in the same sample because the

232   ionization efficiency is compound and solvent specific in electrospray ionization. Also,

233   similar ionization efficiency is assumed for a given OS in different samples as similar

234   retention times are observed and as UHPLC separation resolves most of the matrix

235   components.

236   Blank filters were processed and analyzed in an identical way, and blank

237   correction was made as follows. The presence of targeted quasi-molecular ions in the

238   blanks was systematically verified, and if a chromatographic peak was indeed

239   detected, then it was retained (i.e., considered as real) only if the sample-to-blank

240   ratio of the peak area was greater than 10, with the blank value being subtracted prior

241   to further processing. The DBE value of a molecule reflects the degree of its

242   unsaturation. The DBE value is usually calculated as:

243 $$\text{DBE} = \frac{2c+2+n-h}{2} \qquad \text{(Eq. 1)}$$

244 Not taking into account the two double bonds involved in each sulfate group, the DBE

245 values of OSs calculated by Eq. 1 represent the unsaturation degree of the side carbon

246 chain (eventually bearing oxygen and nitrogen atoms). In addition, one can note that

247 this equation adds one DBE unit for each nitrate group. Molecular formulas with

248 DBE<0 and formulas that disobey the nitrogen rule were discarded. The difference

between the DBE value and the number of N atoms (DBE-n) is the most conservative

criterion to determine whether a compound is aliphatic: the number of OSs with

(DBE-n) < 4 can be regarded as the minimum number of aliphatic OSs (Lin et al.,

2012b).

Both DBE/C and the aromaticity index (AI) could be used as criteria to determine

whether a compound contains aromatic rings with thresholds of DBE/C > 0.67 and

AI > 0.5, respectively. However, AI is more conservative (Koch and Dittmar, 2006).

The value of AI can be calculated according to:

$$AI = \frac{DBE_{AI}}{C_{AI}} = \frac{1+c-o-s-(0.5h)}{c-o-s-n} \qquad (Eq. 2)$$

where DBE_{AI} represents the sum of the minimum number of C=C double bonds and

the number of rings in a formula containing heteroatoms, and C_{AI} represents the

difference between the number of carbon and the number of potential double bonds

caused by heteroatoms. If $DBE_{AI} \leq 0$ or $C_{AI} \leq 0$, then AI is defined to be zero. In

contrast, AI>0.5 and AI≥0.67 indicate the existence of aromatic and fused aromatic

ring structures in a compound, respectively (Koch and Dittmar, 2006).

In the Kendrick mass defect diagram (KMD diagram), CH_2 (14.00000) was

chosen as a base unit. The Kendrick mass (KM_{CH2}) and the Kendrick mass defect

(KMD_{CH2}) can be determined by Eq. 3 and Eq. 4, respectively:

$$KM_{CH_2} = Observed\ Mass \times \left(\frac{14.00000}{14.01565}\right) \quad (Eq. 3)$$

$$KMD_{CH_2} = Nominal\ Mass - KM_{CH_2} \quad (Eq. 4)$$

where "Observed Mass" is the mass measured by the mass spectrometer, and

"Nominal Mass" is the rounded integer mass of a compound.

3. Results and discussion

3.1 Isomers

UHPLC separation was applied prior to MS analysis for detection of potential

isomers hidden behind a given *m/z* value and to provide another dimension of the

ambient aerosol composition complexity. As an example, Figure 2 shows the

extracted ion chromatograms for $C_5H_{10}O_5S$. An OS with this molecular formula has

278   recently been identified in laboratory-generated secondary organic aerosols either

279   from the ozonolysis of isoprene in the presence of sulfate aerosols or from the

280   transformations of isoprene coupled with S(IV)-autoxidation in the aqueous-phase,

281   but only one and two isomers were detected by UPLC-high-resolution mass

282   spectrometers, respectively (Riva et al., 2015a; Szmigielski, 2015). From our ambient

283   samples, 11 isomers were detected in total, with varying numbers of isomers in each

284   sample (see Figure 2 and Table S3). On the other hand, only two isomers were

285   detected in the ambient PM$_{2.5}$ samples from the Diabla Gora rural site (Szmigielski,

286   2015). The reason for this difference in the number of isomers among these studies

287   might arise from the different chromatographic conditions and additional precursors,

288   including different terpenes. In addition, it is difficult to assign which isomers have

289   been detected by Riva et al. (2015a) and Szmigielski (2015) due to different

290   chromatographic conditions and detectors.

291   Additional extracted ion chromatograms are presented in the supplement for

292    $C_5H_{12}O_7S_1$, $C_{10}H_{17}O_7N_1S_1$, and $C_{16}H_{32}O_6S_1$ (Figure S1). Two and four isomers were

293   detected for $C_5H_{12}O_7S_1$ and $C_{10}H_{17}O_7N_1S_1$, respectively, whereas Surratt et al. (2008)

294   detected one and six isomers for these OSs, also from ambient samples. A thorough

295   analysis of UHPLC-Orbitrap MS data leads to the tentative determination of more

296   than 100 CHOS formulas and dozens of CHONS formulas, with various numbers of

297   isomers in each sample. The full list of the neutral mass, molecular formula, number

298   of isomers, retention times, and potential precursors for these assigned OSs is

299   tabulated in Table S3. Having access to the isomeric pattern of significant OSs could

300   be very helpful in the future for identifying possible OS sources. Thus, Table S3

301   provides one of the first data sets of OS isomers in ambient samples.

302   The full mass spectra in summer samples from the three megacities, including all

303   tentatively assigned OSs, have been reconstructed to present the samples' general

304   characteristics. In Figure 3, the X-axis corresponds to the neutral molecular weight of

305   detected OSs, the Y-axis represents their arbitrary abundances, and the number of

306   isomers per detected mass is color-coded. Comparison of the reconstructed mass

307   spectra shows that the number of OSs with an identical formula and the same number

308 of isomers that could be observed in all three megacities accounted for only 17.6% of

309 all the tentatively assigned OS molecular formulas. Between WHS and NJSN, the

310 proportion of OSs sharing identical formulas reached 50.3%, but only 27.9% also

311 possessed the same number of isomers. Quite similarly, between NJSN and

312 SHSD+SHSN, the proportion of OSs sharing identical formulas reached 62.8%, but

313 only 39.4% also had the same number of isomers. Between WHS and SHSD+SHSN,

314 this proportion reached 51.5%, with only 32.3% having the same number of isomers.

315 Therefore, one can consider that the samples from NJ and SH showed greater

316 similarity, especially from their isomeric patterns. This observation is in agreement

317 with the proximity of the two megacities compared to the more distant megacity of

318 WH.

319   As shown in Figure 3, OSs with two to four isomers accounted for about 50% of

320 the total detected OSs. Those with more than six isomers accounted for the largest

321 proportion, and OSs with one isomer were insignificant in WH. In contrast, in SH and

322 NJ, OSs with one isomer only were preponderant, while those with more than six

323 isomers were much less numerous. Clearly, the isomeric pattern differs significantly

324 in WH compared to the other two megacities, probably due to the diversity in

325 precursors and/or oxidation mechanism.

326

327 3.2 Tentative assignment and potential precursors of major OSs

328   The gaseous precursors of many OSs in Figure 3 can be tentatively assigned, since

329 identical formulas of OSs have been observed in chamber studies. In Figure 3, OSs

330 with strong arbitrary intensities have been labeled with a letter as follows: A:

331 $C_5H_8O_3SO_4$; B: $C_5H_{12}O_3SO_4$; C: $C_6H_{10}O_3SO_4$; D: $C_7H_{12}O_3SO_4$; E: $C_9H_{18}O_2SO_4$; F:

332 $C_5H_{11}O_2NO_3SO_4$; G: $C_9H_{16}O_3SO_4$; H: $C_{10}H_{17}NO_3SO_4$; I: $C_5H_{10}O_1(NO_3)_2SO_4$; J:

333 $C_{16}H_{32}O_2SO_4$; and K: $C_{15}H_{25}NO_3SO_4$. Among these OSs, A, C, D, and G are a series

334 of homologues, and so are E and J. A, B, F, and I could be derived from isoprene,

335 whereas D and G could be derived from limonene, C from 3-Z-hexenal, K from

336 β-caryophyllene, and H from various monoterpenes (i.e., α-pinene, β-pinene,

337 α-terpinene and terpinolene) (Chan et al., 2011; Shalamzari et al., 2014; Surratt et al.,

2008; Gomez-Gonzalez et al., 2008). E and J were characterized by high molecular weights and degrees of saturation, presumably being long-chain aliphatic OSs. In general, many abundant OSs could be derived from isoprene, monoterpenes, and sesquiterpenes in these three megacities.

The relative abundance of J was the highest in WH but much lower in the NJSN and SHSD+SHSN samples. H was the highest in the SHSD+SHSN samples, while I was the most abundant in the NJSN sample. It is doubtless that I bears two nitrate groups (two nitrogen atoms in its formula that fulfill the $4s+3n \leq o$ rule) and is the most abundant in the NJSN sample, likely due to active NO_3 radical chemistry at night. F and K, which bear one nitrate group, were also quite abundant in the NJSN sample, underlying the role of NO_3 chemistry at night. The isomer ratios vary from sample to sample and therefore certainly carry information about their origin. These ratios and possible VOC precursors for these most abundant OSs are summarized in Table S4.

3.3 Comparison of OS characteristics

Table 1 summarizes the average characteristics (molecular weight, DBE, and elemental ratios) of tentatively assigned CHOS and CHONS compounds. These CHOS and CHONS compounds were here tentatively regarded as organosulfates and nitrooxy-organosulfates respectively, but other S- and N- containing functional groups could be involved as well in small amount (Lin et al., 2012b). In addition, (o-3s)/c (Tao et al., 2014) and (o-3s-2n)/c have been calculated to illustrate the number of oxygen-containing functional groups per carbon atom. These two values are derived from the fact that each sulfate and nitrate group respectively contains three and two oxygen atoms more than do common oxygen-containing groups, such as a hydroxyl or a carbonyl moiety. (o-3s)/c and (o-3s-2n)/c can therefore be regarded as measures of the degree of oxidation of CHOS and CHONS compounds, respectively.

The average molecular weight and DBE value of CHONS species were generally larger than those of CHOS analogues, because CHONS contains one or two more nitrate groups (the presence of one nitrate group adding one DBE unit). Measurement of the O/C ratio of OSs in Bakersfield (CA, USA) indicated that the degree of

13

368 oxidation of CHONS was larger than that of CHOS throughout the day (O'Brien et al.

369 2014). A similar trend has been observed for $CHONS_1$ and $CHOS_1$ in SH and Los

370 Angeles aerosol samples but using the (o-3)/c ratio to measure the degree of oxidation

371 (Tao et al., 2014). In this study, however, the average degree of oxidation of CHONS

372 was only slightly larger than that of CHOS during the daytime and slightly smaller at

373 night. The use of the (o-3s)/c and (o-3s-2n)/c ratios to evaluate the degrees of

374 oxidation of the CHOS and CHONS carbon chain, respectively, allows for precise

375 comparison of the oxidation states of these two classes of compounds. The values of

376 the oxidation states for OSs and nitrooxy-OSs on a same sample (0.01 to 0.14 units of

377 difference) suggest that the presence of the sulfate and/or nitrate groups is not

378 determinant.

379   The OSs with (DBE-n) < 4 accounted for 86.2, 78.5, and 78.3% of total OSs in WH,

380 NJ, and SH, respectively, suggesting tentatively assigned OSs were mainly aliphatic

381 OSs. Also, the number of OSs with (DBE-n) $\geq$ 4 can be regarded as the maximum

382 number of aromatic OSs. This value appears to be slightly higher in SH (21.7%) and

383 NJ (21.5%) compared to WH (13.8%), possibly indicating a slightly more significant

384 anthropogenic influence for the first two cities.

385   The number of OSs with DBE/C > 0.67 accounted for 2.2, 5.2, and 7.1% of total

386 OSs, and their abundance accounted for 0.6, 1.4, and 8.0% of total abundances of OSs

387 in WHS, NJSD+NJSN, and SHSD+SHSN, respectively. Only a few aromatic OSs

388 with AI > 0.5 were detected, but it could be due to the fact that this value takes into

389 account carbon-bounded S and N but not sulfate and nitrate groups (and the related

390 oxygen atoms), underestimating the aromatic ring content. BS and its analogues were

391 nevertheless detected in most of the samples of the three megacities.

392   Figure 4 shows the CH_2-Kendrick diagrams and Van Krevelen (VK) diagrams for

393 CHOS species for the WHS, NJSD+NJSN, and SHSD+SHSN samples, respectively,

394 and the variation in DBE is color-coded. In the CH_2-Kendrick diagram, compounds in

395 a homologue series of compounds with identical KMD_{CH_2} values form a horizontal

396 line. The molecular formulas of the homologue series 1 and 2, which have DBE

397 values equal to zero, can be written as $C_nH_{2n+2}SO_4$ and $C_nH_{2n+2}O_1SO_4$ (n>4),

398　respectively. Hence, the OS in the homologue series 2 contained one more hydroxyl

399　group or ether group than the corresponding one in the homologue series 1. Similarly,

400　molecular formulas of the homologue series 3, 4, and 7 with DBE=1 can be written as

401　$C_nH_{2n}O_1SO_4$, $C_nH_{2n}O_2SO_4$, and $C_nH_{2n}O_3SO_4$; those for series 6, 9, 11, and 13 with

402　DBE=2 can be written as $C_nH_{2n-2}O_2SO_4$, $C_nH_{2n-2}O_3SO_4$, $C_nH_{2n-2}O_4SO_4$, and

403　$C_nH_{2n-2}O_5SO_4$; and those for series 5, 8, 10, 12, 14, and 15 with DBE=3 can be written

404　as $C_nH_{2n-4}O_1SO_4$, $C_nH_{2n-4}O_2SO_4$, $C_nH_{2n-4}O_3SO_4$, $C_nH_{2n-4}O_4SO_4$, $C_nH_{2n-4}O_5SO_4$, and

405　$C_nH_{2n-4}O_6SO_4$, respectively. For the homologue series with DBE=2 or 3, the oxygen

406　atoms other than those in the sulfate group probably belonged to hydroxyl, carbonyl,

407　or carboxylic groups, because it is unlikely that a compound in this range of

408　molecular weight would contain so many ether groups. CHOS with DBE=4 or 5

409　represented 9.9, 12.2, and 9.5% of the total CHOS species in the WHS, NJSD+NJSN,

410　and SHSD+SHSN samples, respectively.

411　　The region of the CH_2-Kendrick diagrams where KM_{CH_2} is between 350 and 750

412　and KMD_{CH_2} is larger than 0.38 appears to be of particular interest. No CHOS was

413　observed in this region in WHS, whereas up to 6.5 and 9.5% of the total CHOS were

414　detected there in the NJSD+NJSN and SHSD+SHSN samples, respectively. The

415　CHOS species in this region were characterized by a high molecular weight, high

416　degrees of unsaturation and oxidation (DBE > 5 and (o-3s)/c > 0.5), and a minimum

417　amount of isomers (one isomer for 79% of CHOS in this region). Moreover, these

418　CHOS are located in the lower right region of the VK diagrams that plot H/C versus

419　(o-3s)/c ratios (Figure 4, Wu et al. 2004; Kim et al, 2003). They are thus likely to

420　contain one or more aromatic rings (DBE/C > 0.67, but AI<0.5) and come most

421　certainly from anthropogenic precursors.

422　　Fewer CHONS than CHOS species were observed (Figure 5). In the CH_2-Kendrick

423　diagram, the KMD_{CH_2} values of CHONS were generally larger than those of CHOS

424　because of the presence of one or two additional nitrate group contributing to these

425　KMD_{CH_2} values. Similarly to CHOS species, CHONS species in a homologue series

426　with identical KMD_{CH_2} values form a horizontal line. Molecular formulas of the

427　homologue series 1 and 3 with DBE=1 can be written as $C_nH_{2n+1}NO_3SO_4$ and

428 $C_nH_{2n+1}ONO_3SO_4$; those for homologue series 2, 4, 5, and 8 with DBE=2 can be

429 written as $C_nH_{2n-1}NO_3SO_4$, $C_nH_{2n-1}ONO_3SO_4$, $C_nH_{2n-1}O_2NO_3SO_4$, and

430 $C_nH_{2n-1}O_3NO_3SO_4$; those for series 7, 9, and 10 with DBE=3 can be written as

431 $C_nH_{2n-3}O_2NO_3SO_4$, $C_nH_{2n-3}O_3NO_3SO_4$, and $C_nH_{2n-3}O_4NO_3SO_4$; and those for series 6

432 with DBE=4 can be written as $C_nH_{2n-5}ONO_3SO_4$ (n>4). By comparing the molecular

433 formulas of CHOS and CHONS species, it appears that most CHONS could

434 correspond to the addition of nitrate groups on the detected CHOS. In the VK

435 diagrams, the homologue series 1 and 3 constitute upward lines and the other ones

436 constitute downward lines. In the region where KM_{CH2} is between 500 and 700 and

437 KMD_{CH2} is larger than 0.6, CHONS species with DBE values larger than 5, a high

438 molecular weight and a high degree of oxidation ((o-3s-2n)/c > 0.5) were detected in

439 NJSD+NJSN and SHSD+SHSN, but not in WHS. According to the formulas of those

440 CHONS species, their precursors were different from those for any CHOS species. On

441 the other hand, a few additional CHONS species with DBE values also larger than 5,

442 relatively low molecular weight and low degrees of saturation and oxidation

443 ((o-3s-2n)/c < 0.3) were present in the three megacities.

444   Figure S2 shows the numbers of CHOS and CHONS species in different mass

445 ranges. Generally, OSs in the mass range of 250–300 Da showed the greatest variety.

446 The number of OSs in the mass range of 200–400 Da accounted for 90.5, 83.1, and

447 85.4% of determined OSs in WHS, NJSD+NJSN, and SHSD+SHSN, respectively.

448 OSs with molecular weights larger than 500 Da characterized by high degrees of

449 unsaturation in the KMD diagrams existed in the NJ and SH samples, whereas the

450 molecular weight of all OSs in the WHS sample was less than 500 Da. In summary,

451 the molecular characteristics of tentatively assigned OSs between NJSD+NJSN and

452 SHSD+SHSN shared better similarity, probably because NJ and SH are

453 geographically closer at the lower reach of the Yangtze River, whereas WH is at the

454 middle reach of the Yangtze River.

455

456 3.4 Formation pathways of isoprene-derived OSs in the three megacities

457   Isoprene has been shown to be an important precursor of OSs in the three

458   megacities. Previous studies suggest that IEPOX ($C_5H_{10}O_3$) and MAE ($C_4H_6O_3$) are

459   two key reactive intermediates that are formed during isoprene oxidation under low-

460   and high-NO_x conditions, respectively. Subsequent acid catalyzed-reactions of IEPOX

461   and MAE in the presence of sulfates lead to the formation of $C_5H_{12}O_3SO_4$ and

462   $C_4H_8O_3SO_4$, respectively (Surratt et al., 2010; Worton et al., 2013), with the C_4 OS

463   being promoted under high-NO_x conditions compared to the C_5 OS. C_5 and C_4 OSs

464   could also be formed from sulfate/sulfite radical-induced oxidation reactions with

465   isoprene and its oxidation products (i.e., methyl vinyl ketone, and methacrolein) in the

466   aqueous phase, respectively (Schone et al., 2014; Noziere et al., 2010). Since the

467   liquid water content is not available for our ambient samples, these aqueous reaction

468   pathways are not considered here.

469   In this study, the S/C ratio has been limited to 0–0.2 to assure that the obtained

470   compound exists in nature (Lin et al., 2012a; Tao et al., 2014; Wozniak et al., 2008).

471   As a result, $C_4H_8O_3SO_4$ has been eliminated by this criterion. Manually extracted

472   ratios of the abundances of $C_4H_8O_3SO_4$ to $C_5H_{12}O_3SO_4$ (denoted hereafter as C_4/C_5

473   ratios) were used to elucidate the major formation pathway of isoprene-derived OSs in

474   the three megacities.

475   In SH winter daytime samples, the C_4/C_5 ratio was 8.9 and decreased to 0.20

476   during summer. In WH, the C_4/C_5 ratio was equal to 0.22 in winter and 0.13 in

477   summer. In both cases, these observations are consistent with the C_4 OS being

478   promoted with higher winter NO_x levels but also suggest that even in winter, isoprene

479   OSs are formed under low-NO_x conditions. In the NJSD sample, the C_4/C_5 ratio was

480   about 2.5, suggesting that the high-NO_x pathway might dominate in summer in NJ

481   (Dong et al., 2013).

482

483   3.5 Comparison of OSs in the SH samples

484   For a more accurate comparison, the abundance of $C_{10}H_{17}NO_3SO_4$ in the SHSN

485   sample (the highest one from all the SH samples) was set arbitrarily to 100%, and an

486   abundance limit corresponding to 0.5% of this value was used to include or exclude

487   the OSs from the four SH samples in the following comparison. Figure 6 shows that

the number of OSs in the SHSD and SHSN samples was much larger than those in the SHWD and SHWN samples, respectively, consistent with a higher photochemical activity and/or higher precursor emissions in summer than in winter. The number of OSs in the SHSN and SHWN samples, especially the number of CHONS, was much larger than that in the SHSD and SHWD samples, respectively, consistent with the previous observation in Figure 3 (see section 3.2) that much more CHONS is present during nighttime.

As shown in Figure 7, the total arbitrary abundances of OSs in the SHSD and SHSN samples were 2.1 and 3.0 times higher than in the SHWD and SHWN samples. The total arbitrary abundances of CHOS did not display significant differences between SHSD and SHSN or between SHWD and SHWN. However, the arbitrary abundances of CHONS in these SHSN and SHWN samples were 5.0 times and 2.2 times higher than in the SHSD and SHWD samples. This is consistent with an expected nighttime chemistry of NO_3. Moreover, the variety (Figure 6) and the abundance (Figure 7) of CHONS in both the SHWN and SHSN samples were far larger than those in SHWD and SHSD.

The fact that the SHSN sample showed a higher abundance and variety of CHONS than the SHWD sample seems to point toward a CHONS formation driven by both daytime photochemistry (and/or precursor emission) and subsequent nighttime NO_3 chemistry. Similar trends of higher CHONS abundance during nighttime than during daytime were observed in Beijing, China (van Pinxteren et al., 2009), Atlanta, GA (Hatch et al., 2011), and Bakersfield, CA, USA (O'Brien et al., 2014). However, He et al. (2014) observed a reverse trend at a regional background site in the Pearl River Delta region (concentrations of nitrooxy-OSs were higher during daytime), concluding that photochemical reactions could also lead to the formation of a significant amount of nitrooxy-OSs. This photochemical pathway could contribute to the formation of the nitrooxy-OSs detected during daytime, even if they showed only relatively low abundances in this study.

Figure 7 shows the carbon number-based arbitrary abundance of CHOS and CHONS. In all four samples, more than 60% of the OSs were characterized by 5 to 10

518 carbon atom chains. In the SHSD and SHSN samples, C_5 and C_{10} were the most

519 abundant. Isoprene and monoterpenes could be the main precursors for most of the C_5

520 and C_{10} OSs (Riva et al., 2015a; Surratt et al., 2008). On the other hand, a recent work

521 (Riva et al., 2015b) suggests that a number of observed C_{10} OSs (e.g., $C_{10}H_{12}O_7S_1$)

522 might be derived from PAHs. In addition to C_5 and C_{10}, the relative abundances of C_8,

523 C_9, and C_{14+} were also high in the SHWD and SHWN samples, hinting at additional

524 precursors. In contrast, C_{10} derived from monoterpenes always represented the

525 dominant category in spring, autumn, and winter in the Pearl River Delta, South

526 China, and in Taiwan (Lin et al., 2012b), underlying a lesser anthropogenic influence

527 in these two regions than in the Yangtze River region.

528   The VK diagrams of CHOS and CHONS in the SH samples are presented in

529 Figure S3, which represents a combination of Figure 4 and Figure 5 (with a lesser

530 number of OSs accounted for). OSs in the four samples were characterized by similar

531 degrees of saturation. OSs with a low degree of saturation and a high molecular

532 weight existed in all four samples. Table 1 and Figure S3 show that the average

533 degree of oxidation of OSs in the SHSD and SHSN samples was higher than those in

534 the SHWD and SHWN samples, which is consistent with a promoted photochemical

535 activity in summer.

536

537 4. Conclusions

538   In this study, atmospheric PM$_{2.5}$ samples in WH, NJ, and SH were analyzed using

539 an UHPLC-Orbitrap mass spectrometer. More than 100 formulas of CHOS and

540 dozens of formulas of CHONS with various numbers of isomers were tentatively

541 determined in each sample. These CHOS and CHONS compounds were here

542 tentatively regarded as organosulfates and nitrooxy-organosulfates, respectively.

543   Aliphatic OSs represented at least 78% of the tentatively determined OSs in the

544 three megacity summer samples, while there was much less aromatic OSs.

545 Comparison of the molecular formula, number of isomers, average molecular weight,

546 and degrees of saturation and oxidation suggests that OSs in aerosol samples from NJ

547 and SH shared more similarities.

Major OSs in these ambient samples could be derived from biogenic precursors (isoprene, monoterpenes, and sesquiterpenes), but also from PAHs. Isoprene appeared to be most likely one of the important precursors in the three megacities, and the influence of NO_x level on the nature of isoprene-derived OSs is consistent with the literature. Clearly, the identity, precursors, and formation mechanisms of many OSs have yet to be positively elucidated. The systematic use of chromatographic separation prior to MS detection appears essential given the variety of the precursors and the resulting isomers.

References:

Andreae, M. O. and Crutzen, P. J.: Atmospheric aerosols: Biogeochemical sources and role in atmospheric chemistry, Science, 276, 1052-1058, doi:10.1126/science.276.5315.1052, 1997.

Chan, M. N., Surratt, J. D., Chan, A. W. H., Schilling, K., Offenberg, J. H., Lewandowski, M., Edney, E. O., Kleindienst, T. E., Jaoui, M., Edgerton, E. S., Tanner, R. L., Shaw, S. L., Zheng, M., Knipping, E. M., and Seinfeld, J. H.: Influence of aerosol acidity on the chemical composition of secondary organic aerosol from beta-caryophyllene, Atmos. Chem. Phys., 11, 1735-1751, doi:10.5194/acp-11-1735-2011, 2011.

Darer, A. I., Cole-Filipiak, N. C., O'Connor, A. E., and Elrod, M. J.: Formation and stability of atmospherically relevant isoprene-derived organosulfates and organonitrates, Environ. Sci. Technol., 45, 1895-1902, doi:10.1021/es103797z, 2011.

Dong, X. Y., Gao, Y., Fu, J. S., Li, J., Huang, K., Zhuang, G. S., and Zhou, Y.: Probe into gaseous pollution and assessment of air quality benefit under sector dependent emission control strategies over megacities in Yangtze River Delta, China, Atmos. Environ., 79, 841-852, doi:10.1016/j.atmosenv.2013.07.041, 2013.

El Haddad, I., Marchand, N., D'Anna, B., Jaffrezo, J.-L., and Wortham, H.: Functional group composition of organic aerosol from combustion emissions and secondary processes at two contrasted urban environments, Atmos. Environ., 75, 308-320, doi:10.1016/j.atmosenv.2013.04.019, 2013.

Fuller, S. J., Zhao, Y. J., Cliff, S. S., Wexler, A. S., and Kalberer, M.: Direct surface analysis of

587   time-resolved aerosol impactor samples with ultrahigh-resolution mass spectrometry, Anal. Chem.,
588   84, 9858-9864, doi:10.1021/ac3020615, 2012.

589   Gomez-Gonzalez, Y., Surratt, J. D., Cuyckens, F., Szmigielski, R., Vermeylen, R., Jaoui, M.,
590   Lewandowski, M., Offenberg, J. H., Kleindienst, T. E., Edney, E. O., Blockhuys, F., Van Alsenoy, C.,
591   Maenhaut, W., and Claeys, M.: Characterization of organosulfates from the photooxidation of
592   isoprene and unsaturated fatty acids in ambient aerosol using liquid chromatography/(-) electrospray
593   ionization mass spectrometry, J. Mass Spectrom., 43, 371-382, doi:10.1002/jms.1329, 2008.

594   Guenther, A., Hewitt, C. N., Erickson, D., Fall, R., Geron, C., Graedel, T., Harley, P., Klinger, L.,
595   Lerdau, M., McKay, W. A., Pierce, T., Scholes, B., Steinbrecher, R., Tallamraju, R., Taylor, J., and
596   Zimmerman, P.: A global-model of natural volatile organic-compound emissions, J. Geophys. Res.
597   Atmos., 100, 8873-8892, doi:10.1029/94jd02950, 1995.

598   Hallquist, M., Wenger, J. C., Baltensperger, U., Rudich, Y., Simpson, D., Claeys, M., Dommen, J.,
599   Donahue, N. M., George, C., Goldstein, A. H., Hamilton, J. F., Herrmann, H., Hoffmann, T., Iinuma,
600   Y., Jang, M., Jenkin, M. E., Jimenez, J. L., Kiendler-Scharr, A., Maenhaut, W., McFiggans, G.,
601   Mentel, T. F., Monod, A., Prevot, A. S. H., Seinfeld, J. H., Surratt, J. D., Szmigielski, R., and Wildt,
602   J.: The formation, properties and impact of secondary organic aerosol: current and emerging issues,
603   Atmos. Chem. Phys., 9, 5155-5236, doi:10.5194/acp-9-5155-2009, 2009.

604   Hatch, L. E., Creamean, J. M., Ault, A. P., Surratt, J. D., Chan, M. N., Seinfeld, J. H., Edgerton, E. S.,
605   Su, Y. X., and Prather, K. A.: Measurements of isoprene-derived organosulfates in ambient aerosols
606   by aerosol time-of-flight mass spectrometry-Part 2: Temporal variability and formation mechanisms,
607   Environ. Sci. Technol., 45, 8648-8655, doi:10.1021/es2011836, 2011.

608   Hawkins, L. N., Russell, L. M., Covert, D. S., Quinn, P. K., and Bates, T. S.: Carboxylic acids, sulfates,
609   and organosulfates in processed continental organic aerosol over the southeast Pacific Ocean during
610   VOCALS-REx 2008, J. Geophys. Res. Atmos., 115, D13201, doi:10.1029/2009jd013276, 2010.

611   He, Q. F., Ding, X., Wang, X. M., Yu, J. Z., Fu, X. X., Liu, T. Y., Zhang, Z., Xue, J., Chen, D. H.,
612   Zhong, L. J., and Donahue, N. M.: Organosulfates from pinene and isoprene over the Pearl River
613   Delta, south China: Seasonal variation and implication in formation mechanisms, Environ. Sci.
614   Technol., 48, 9236-9245, doi:10.1021/es501299v, 2014.

615   Hu, K. S., Darer, A. I., and Elrod, M. J.: Thermodynamics and kinetics of the hydrolysis of
616   atmospherically relevant organonitrates and organosulfates, Atmos. Chem. Phys., 11, 8307-8320,
617   doi:10.5194/acp-11-8307-2011, 2011.

618   Huang, C., Chen, C. H., Li, L., Cheng, Z., Wang, H. L., Huang, H. Y., Streets, D. G., Wang, Y. J.,
619   Zhang, G. F., and Chen, Y. R.: Emission inventory of anthropogenic air pollutants and VOC species
620   in the Yangtze River Delta region, China, Atmos. Chem. Phys., 11, 4105-4120,
621   doi:10.5194/acp-11-4105-2011, 2011.

622   Iinuma, Y., Muller, C., Berndt, T., Boge, O., Claeys, M., and Herrmann, H.: Evidence for the existence
623   of organosulfates from beta-pinene ozonolysis in ambient secondary organic aerosol, Environ. Sci.
624   Technol., 41, 6678-6683, doi:10.1021/es070938t, 2007a.

625   Iinuma, Y., Muller, C., Boge, O., Gnauk, T., and Herrmann, H.: The formation of organic sulfate esters
626   in the limonene ozonolysis secondary organic aerosol (SOA) under acidic conditions, Atmos.
627   Environ., 41, 5571-5583, doi:10.1016/j.atmosenv.2007.03.007, 2007b.

628   Kahnt, A., Behrouzi, S., Vermeylen, R., Shalamzari, M. S., Vercauteren, J., Roekens, E., Claeys, M.,
629   and Maenhaut, W.: One-year study of nitro-organic compounds and their relation to wood burning in
630   PM_{10} aerosol from a rural site in Belgium, Atmos. Environ., 81, 561-568,

631   doi:10.1016/j.atmosenv.2013.09.041, 2013.

632   Kim, S., Kramer, R. W., and Hatcher, P. G.: Graphical method for analysis of ultrahigh-resolution
633   broadband mass spectra of natural organic matter, the van Krevelen diagram, Anal. Chem., 75,
634   5336-5344, doi:10.1021/ac034415p, 2003.

635   Koch, B. P. and Dittmar, T.: From mass to structure: An aromaticity index for high-resolution mass data
636   of natural organic matter, Rapid Commun. Mass Sp., 20, 926-932, doi:10.1002/rcm.2386, 2006.

637   Kristensen, K. and Glasius, M.: Organosulfates and oxidation products from biogenic hydrocarbons in
638   fine aerosols from a forest in North West Europe during spring, Atmos. Environ., 45, 4546-4556,
639   doi:10.1016/j.atmosenv.2011.05.063, 2011.

640   Kundu, S., Quraishi, T. A., Yu, G., Suarez, C., Keutsch, F. N., and Stone, E. A.: Evidence and
641   quantitation of aromatic organosulfates in ambient aerosols in Lahore, Pakistan, Atmos. Chem. Phys.,
642   13, 4865-4875, doi:10.5194/acp-13-4865-2013, 2013.

643   Liggio, J., Li, S. M., and McLaren, R.: Heterogeneous reactions of glyoxal on particulate matter:
644   Identification of acetals and sulfate esters, Environ. Sci. Technol., 39, 1532-1541,
645   doi:10.1021/es048375y, 2005.

646   Lin, P., Rincon, A. G., Kalberer, M., and Yu, J. Z.: Elemental composition of HULIS in the Pearl River
647   Delta region, China: Results inferred from positive and negative electrospray high resolution mass
648   spectrometric data, Environ. Sci. Technol., 46, 7454-7462, doi:10.1021/es300285d, 2012a.

649   Lin, P., Yu, J. Z., Engling, G., and Kalberer, M.: Organosulfates in humic-like substance fraction
650   isolated from aerosols at seven locations in East Asia: A study by ultra-high-resolution mass
651   spectrometry, Environ. Sci. Technol., 46, 13118-13127, doi:10.1021/es303570v, 2012b.

652   Lin, Y. H., Zhang, Z., Docherty, K. S., Zhang, H., Budisulistiorini, S. H., Rubitschun, C. L., Shaw, S. L.,
653   Knipping, E. M., Edgerton, E. S., Kleindienst, T. E., Gold, A., and Surratt, J. D.: Isoprene epoxydiols
654   as precursors to secondary organic aerosol formation: acid-catalyzed reactive uptake studies with
655   authentic compounds, Environ. Sci. Technol., 46, 250-258, doi:10.1021/es202554c, 2012c.

656   Lin, Y. H., Zhang, H. F., Pye, H. O. T., Zhang, Z. F., Marth, W. J., Park, S., Arashiro, M., Cui, T. Q.,
657   Budisulistiorini, H., Sexton, K. G., Vizuete, W., Xie, Y., Luecken, D. J., Piletic, I. R., Edney, E. O.,
658   Bartolotti, L. J., Gold, A., and Surratt, J. D.: Epoxide as a precursor to secondary organic aerosol
659   formation from isoprene photooxidation in the presence of nitrogen oxides, P. Natl. Acad. Sci. USA,
660   110, 6718-6723, doi:10.1073/pnas.1221150110, 2013.

661   Ma, Y., Chen, J. M., and Wang, L.: Characteristics and formation mechanisms of atmospheric
662   organosulfates, Prog. Chem., 24, 2277-2286, 2012.

663   Ma, Y., Xu, X. K., Song, W. H., Geng, F. H., and Wang, L.: Seasonal and diurnal variations of
664   particulate organosulfates in urban Shanghai, China, Atmos. Environ., 85, 152-160,
665   doi:10.1016/j.atmosenv.2013.12.017, 2014.

666   Magari, S. R., Schwartz, J., Williams, P. L., Hauser, R., Smith, T. J., and Christiani, D. C.: The
667   association of particulate air metal concentrations with heart rate variability, Environ. Health
668   Perspect., 110, 875-880, 2002.

669   Noziere, B., Ekstrom, S., Alsberg, T., and Holmstrom, S.: Radical-initiated formation of organosulfates
670   and surfactants in atmospheric aerosols, Geophys. Res. Lett., 37, doi:10.1029/2009gl041683, 2010.

671   O'Brien, R. E., Laskin, A., Laskin, J., Rubitschun, C. L., Surratt, J. D., and Goldstein, A. H.: Molecular
672   characterization of S- and N-containing organic constituents in ambient aerosols by negative ion
673   mode high-resolution nanospray desorption electrospray ionization mass spectrometry: CalNex 2010
674   field study, J. Geophys. Res. Atmos., 119, 12706-12720, doi:10.1002/2014jd021955, 2014.

675 Olson, C. N., Galloway, M. M., Yu, G., Hedman, C. J., Lockett, M. R., Yoon, T., Stone, E. A., Smith, L.
676   M., and Keutsch, F. N.: Hydroxycarboxylic acid-derived organosulfates: synthesis, stability, and
677   quantification in ambient aerosol, Environ. Sci. Technol., 45, 6468-6474, doi:10.1021/es201039p,
678   2011.

679 Ostro, B., Feng, W. Y., Broadwin, R., Green, S., and Lipsett, M.: The effects of components of fine
680   particulate air pollution on mortality in California: Results from CALFINE, Environ. Health
681   Perspect., 115, 13-19, doi:10.1289/ehp.9281, 2007.

682 Paulot, F., Crounse, J. D., Kjaergaard, H. G., Kurten, A., St Clair, J. M., Seinfeld, J. H., and Wennberg,
683   P. O.: Unexpected epoxide formation in the gas-phase photooxidation of isoprene, Science, 325,
684   730-733, doi:10.1126/science.1172910, 2009.

685 Riva, M., Budisulistiorini, S. H., Zhang, Z., Gold, A., and Surratt, J. D.: Chemical characterization of
686   secondary organic aerosol constituents from isoprene ozonolysis in the presence of acidic aerosol,
687   Atmos. Environ., doi:10.1016/j.atmosenv.2015.06.027, 2015a.

688 Riva, M., Tomaz, S., Cui, T., Lin, Y.-H., Perraudin, E., Gold, A., Stone, E. A., Villenave, E., and Surratt,
689   J. D.: Evidence for an unrecognized secondary anthropogenic source of organosulfates and
690   sulfonates: Gas-phase oxidation of polycyclic aromatic hydrocarbons in the presence of sulfate
691   aerosol, Environ. Sci. Technol., 49, 6654-6664, doi:10.1021/acs.est.5b00836, 2015b.

692 Rudzinski, K. J., Gmachowski, L., and Kuznietsova, I.: Reactions of isoprene and sulphoxy
693   radical-anions - a possible source of atmospheric organosulphites and organosulphates, Atmos.
694   Chem. Phys., 9, 2129-2140, 2009.

695 Schindelka, J., Iinuma, Y., Hoffmann, D., and Herrmann, H.: Sulfate radical-initiated formation of
696   isoprene-derived organosulfates in atmospheric aerosols, Faraday Discussions, 165, 237-259,
697   doi:10.1039/c3fd00042g, 2013.

698 Schone, L., Schindelka, J., Szeremeta, E., Schaefer, T., Hoffmann, D., Rudzinski, K. J., Szmigielski, R.,
699   and Herrmann, H.: Atmospheric aqueous phase radical chemistry of the isoprene oxidation products
700   methacrolein, methyl vinyl ketone, methacrylic acid and acrylic acid--kinetics and product studies,
701   Phys. Chem. Chem. Phys., 16, 6257-6272, doi:10.1039/c3cp54859g, 2014.

702 Shalamzari, M. S., Kahnt, A., Vermeylen, R., Kleindienst, T. E., Lewandowski, M., Cuyckens, F.,
703   Maenhaut, W., and Claeys, M.: Characterization of polar organosulfates in secondary organic
704   aerosol from the green leaf volatile 3-Z-hexenal, Environ. Sci. Technol., 48, 12671-12678,
705   doi:10.1021/es503226b, 2014.

706 Staudt, S., Kundu, S., Lehmler, H. J., He, X. R., Cui, T. Q., Lin, Y. H., Kristensen, K., Glasius, M.,
707   Zhang, X. L., Weber, R. J., Surratt, J. D., and Stone, E. A.: Aromatic organosulfates in atmospheric
708   aerosols: Synthesis, characterization, and abundance, Atmos. Environ., 94, 366-373,
709   doi:10.1016/j.atmosenv.2014.05.049, 2014.

710 Stone, E. A., Hedman, C. J., Sheesley, R. J., Shafer, M. M., and Schauer, J. J.: Investigating the
711   chemical nature of humic-like substances (HULIS) in North American atmospheric aerosols by
712   liquid chromatography tandem mass spectrometry, Atmos. Environ., 43, 4205-4213,
713   doi:10.1016/j.atmosenv.2009.05.030, 2009.

714 Surratt, J. D., Kroll, J. H., Kleindienst, T. E., Edney, E. O., Claeys, M., Sorooshian, A., Ng, N. L.,
715   Offenberg, J. H., Lewandowski, M., Jaoui, M., Flagan, R. C., and Seinfeld, J. H.: Evidence for
716   organosulfates in secondary organic aerosol, Environ. Sci. Technol., 41, 517-527,
717   doi:10.1021/es062081q, 2007.

718 Surratt, J. D., Gomez-Gonzalez, Y., Chan, A. W. H., Vermeylen, R., Shahgholi, M., Kleindienst, T. E.,

719   Edney, E. O., Offenberg, J. H., Lewandowski, M., Jaoui, M., Maenhaut, W., Claeys, M., Flagan, R.
720   C., and Seinfeld, J. H.: Organosulfate formation in biogenic secondary organic aerosol, J. Phys.
721   Chem. A, 112, 8345-8378, doi:10.1021/jp802310p, 2008.

722   Surratt, J. D., Chan, A. W. H., Eddingsaas, N. C., Chan, M. N., Loza, C. L., Kwan, A. J., Hersey, S. P.,
723   Flagan, R. C., Wennberg, P. O., and Seinfeld, J. H.: Reactive intermediates revealed in secondary
724   organic aerosol formation from isoprene, P. Natl. Acad. Sci. USA, 107, 6640-6645,
725   doi:10.1073/pnas.0911114107, 2010.

726   Szmigielski, R.: Evidence for C_5 organosulfur secondary organic aerosol components from in-cloud
727   processing of isoprene: Role of reactive SO_4 and SO_3 radicals, Atmos. Environ.,
728   doi:10.1016/j.atmosenv.2015.10.072, 2015.

729   Tao, S., Lu, X., Levac, N., Bateman, A. P., Nguyen, T. B., Bones, D. L., Nizkorodov, S. A., Laskin, J.,
730   Laskin, A., and Yang, X.: Molecular characterization of organosulfates in organic aerosols from
731   Shanghai and Los Angeles urban areas by nanospray-desorption electrospray ionization
732   high-resolution mass spectrometry, Environ. Sci. Technol., 48, 10993-11001, doi:10.1021/es5024674,
733   2014.

734   Tolocka, M. P. and Turpin, B.: Contribution of organosulfur compounds to organic aerosol mass,
735   Environ. Sci. Technol., 46, 7978-7983, doi:10.1021/es300651v, 2012.

736   van Pinxteren, D., Bruggemann, E., Gnauk, T., Iinuma, Y., Muller, K., Nowak, A., Achtert, P.,
737   Wiedensohler, A., and Herrmann, H.: Size- and time-resolved chemical particle characterization
738   during CAREBeijing-2006: Different pollution regimes and diurnal profiles, J. Geophys. Res.
739   Atmos., 114, D00g09, doi:10.1029/2008jd010890, 2009.

740   Wang, L., Du, H. H., Chen, J. M., Zhang, M., Huang, X. Y., Tan, H. B., Kong, L. D., and Geng, F. H.:
741   Consecutive transport of anthropogenic air masses and dust storm plume: Two case events at
742   Shanghai, China, Atmos. Res., 127, 22-33, doi:10.1016/j.atmosres.2013.02.011, 2013.

743   Worton, D. R., Surratt, J. D., LaFranchi, B. W., Chan, A. W. H., Zhao, Y. L., Weber, R. J., Park, J. H.,
744   Gilman, J. B., de Gouw, J., Park, C., Schade, G., Beaver, M., St Clair, J. M., Crounse, J., Wennberg,
745   P., Wolfe, G. M., Harrold, S., Thornton, J. A., Farmer, D. K., Docherty, K. S., Cubison, M. J.,
746   Jimenez, J. L., Frossard, A. A., Russell, L. M., Kristensen, K., Glasius, M., Mao, J. Q., Ren, X. R.,
747   Brune, W., Browne, E. C., Pusede, S. E., Cohen, R. C., Seinfeld, J. H., and Goldstein, A. H.:
748   Observational insights into aerosol formation from isoprene, Environ. Sci. Technol., 47,
749   11403-11413, doi:10.1021/es4011064, 2013.

750   Wozniak, A. S., Bauer, J. E., Sleighter, R. L., Dickhut, R. M., and Hatcher, P. G.: Technical Note:
751   Molecular characterization of aerosol-derived water soluble organic carbon using ultrahigh
752   resolution electrospray ionization Fourier transform ion cyclotron resonance mass spectrometry,
753   Atmos. Chem. Phys., 8, 5099-5111, doi:10.5194/acp-8-5099-2008, 2008.

754   Wu, Z. G., Rodgers, R. P., and Marshall, A. G.: Two- and three-dimensional van Krevelen diagrams: A
755   graphical analysis complementary to the Kendrick mass plot for sorting elemental compositions of
756   complex organic mixtures based on ultrahigh-resolution broadband Fourier transform ion cyclotron
757   resonance mass measurements, Anal. Chem., 76, 2511-2516, doi:10.1021/ac0355449, 2004.

758   Xiao, S., Wang, M. Y., Yao, L., Kulmala, M., Zhou, B., Yang, X., Chen, J. M., Wang, D. F., Fu, Q. Y.,
759   Worsnop, D. R., and Wang, L.: Strong atmospheric new particle formation in winter in urban
760   Shanghai, China, Atmos. Chem. Phys., 15, 1769-1781, doi:10.5194/acp-15-1769-2015, 2015.

761   Zhang, H. F., Worton, D. R., Lewandowski, M., Ortega, J., Rubitschun, C. L., Park, J. H., Kristensen,
762   K., Campuzano-Jost, P., Day, D. A., Jimenez, J. L., Jaoui, M., Offenberg, J. H., Kleindienst, T. E.,

763   Gilman, J., Kuster, W. C., de Gouw, J., Park, C., Schade, G. W., Frossard, A. A., Russell, L., Kaser,

764   L., Jud, W., Hansel, A., Cappellin, L., Karl, T., Glasius, M., Guenther, A., Goldstein, A. H., Seinfeld,

765   J. H., Gold, A., Kamens, R. M., and Surratt, J. D.: Organosulfates as tracers for secondary organic

766   aerosol (SOA) formation from 2-Methyl-3-Buten-2-ol (MBO) in the atmosphere, Environ. Sci.

767   Technol., 46, 9437-9446, doi:10.1021/es301648z, 2012.

768   Zheng, J., Ma, Y., Chen, M. D., Zhang, Q., Wang, L., Khalizov, A. F., Yao, L., Wang, Z., Wang, X., and

769   Chen, L. X.: Measurement of atmospheric amines and ammonia using the high resolution

770   time-of-flight chemical ionization mass spectrometry, Atmos. Environ., 102, 249-259,

771   doi:10.1016/j.atmosenv.2014.12.002, 2015.

Table 1．Summary of sampling location, sampling time, molecular weight (MW), double bond equivalents (DBE), and elemental ratios (arithmetic mean ± standard deviation) of tentatively assigned CHOS and CHONS.

Location	Sample ID	Sampling time	Number of formulas (CHOS/CHONS)	CHOS [a]				CHONS [b]			
				MW	DBE	(o-3s)/c [c]	H/C [d]	MW	DBE	(o-3s-2n)/c [e]	H/C
Wuhan	WHW	9:00 a.m., Jan. 26 - 9:00 a.m., Jan 27, 2012	149/43	266.6±57.2	2.56±2.60	0.37±0.25	1.68±0.44	311.0±60.5	3.61±2.57	0.35±0.13	1.58±0.46
	WHS	8:30 a.m., Jun. 15 - 8:30 a.m., Jun. 16, 2012	213/55	287.9±60.8	2.16±1.64	0.39±0.23	1.75±0.36	318.1±53.8	2.98±1.52	0.40±0.17	1.69±0.34
Nanjing	NJSD	7:30 a.m. - 7:30 p.m., Aug. 29, 2012	139/54	288.9±67.9	1.82±1.32	0.39±0.25	1.83±0.27	313.6±48.2	2.56±1.08	0.44±0.21	1.79±0.23
	NJSN	7:30 p.m., Aug. 29 - 7:30 a.m., Aug. 30, 2012	160/72	294.0±97.3	3.21±3.84	0.46±0.34	1.65±0.45	335.2±74.3	3.46±2.30	0.43±0.20	1.66±0.37
	NJSD+NJSN	Combination [f]	205/83	304.8±93.5	3.00±3.47	0.43±0.32	1.68±0.41	332.5±70.7	3.28±2.21	0.44±0.21	1.69±0.35
Shanghai	SHWD	7:30 a.m. - 7:30 p.m., Jan. 17, 2013	125/32	274.3±81.1	2.38±2.56	0.39±0.31	1.72±0.46	328.7±132.2	4.22±3.95	0.44±0.33	1.53±0.57
	SHWN	7:30 p.m., Jan. 17 - 7:30 a.m., Jan. 18, 2013	159/54	270.0±71.1	2.54±2.39	0.40±0.29	1.69±0.44	303.9±51.9	2.98±2.50	0.38±0.17	1.71±0.46
	SHWD+SHWN	Combination [f]	168/59	277.2±71.2	2.63±2.59	0.40±0.29	1.68±0.46	325.8±92.0	3.59±3.50	0.42±0.27	1.64±0.52
	SHSD	8:00 a.m. - 8:00 p.m., Jul. 28, 2013	165/40	296.4±84.7	2.76±2.66	0.47±0.32	1.68±0.42	348.2±115.4	4.03±3.48	0.61±0.43	1.55±0.52
	SHSN	8:00 p.m., Jul. 28 - 8:00 a.m., Jul. 29, 2013.	122/51	278.1±73.9	2.36±2.48	0.48±0.29	1.74±0.40	319.2±73.0	3.26±2.93	0.45±0.22	1.69±0.44
	SHSD+SHSN	Combination [f]	168/58	296.3±84.7	2.77±2.65	0.47±0.31	1.68±0.42	337.6±102.2	3.52±3.04	0.53±0.38	1.64±0.47

[a] Molecules with (o-4s)/c<0 were not included.

[b] Molecules with (o-4s-3n)/c<0 were not included.

[c] (o-3s)/c infers to the extent of oxidation for a CHOS molecule.

[d] H/C refers to the ratio between hydrogen atom and carbon atom in a molecule.

[e] (o-3s-2n)/c refers to the extent of oxidation for a CHONS molecule.

[f] Combination of two samples for a comparison purpose.

Figure Captions

Figure 1. Locations of Wuhan (WH), Nanjing (NJ), and Shanghai (SH) in China.

Figure 2. LC chromatograms of tentatively determined $C_5H_{10}O_5S_1$ (potentially from isoprene). A chromatogram for the NJSD sample is not included because a large amount of sample injection led to corruption of peaks and hence inaccurate retention times and worse peak resolution.

Figure 3. Mass spectra of detected CHOS and CHONS reconstructed from extracted ion chromatograms (UHPLC-Orbitrap MS analysis, negative ionization mode). X-axis corresponds to the molecular weight (Da) of the identified species. The number of isomers for a given formula is marked by colors. A, neutral mass = 211.9993 Da, $C_5H_8O_7S_1$; B, neutral mass=216.0306 Da, $C_5H_{12}O_7S_1$; C, neutral mass=226.0150 Da, $C_6H_{10}O_7S_1$; D, neutral mass=240.0307 Da, $C_7H_{12}O_7S_1$; E, neutral mass=254.0827 Da, $C_9H_{18}O_6S_1$; F, neutral mass=261.0157 Da, $C_5H_{11}O_9N_1S_1$; G, neutral mass=268.0620 Da, $C_9H_{16}O_7S_1$; H, neutral mass=295.0729 Da, $C_{10}H_{17}O_7N_1S_1$; I, neutral mass=306.0007 Da, $C_5H_{10}O_{11}N_2S_1$; J, neutral mass=352.1922 Da, $C_{16}H_{32}O_6S_1$; K, neutral mass=363.1356 Da, $C_{15}H_{25}O_7N_1S_1$.

Figure 4. (a–c) CH_2-Kendrick diagrams and (d–e) Van Krevelen diagrams for CHOS. The color-coding indicates the DBE values calculated from Eq. 1. The molecular formulas of the homologue series 1 to 15 can be written as $C_nH_{2n+2}SO_4$, $C_nH_{2n+2}O_1SO_4$, $C_nH_{2n}O_1SO_4$, $C_nH_{2n}O_2SO_4$, $C_nH_{2n-4}O_1SO_4$, $C_nH_{2n-2}O_2SO_4$, $C_nH_{2n}O_3SO_4$, $C_nH_{2n-4}O_2SO_4$, $C_nH_{2n-2}O_3SO_4$, $C_nH_{2n-4}O_3SO_4$, $C_nH_{2n-2}O_4SO_4$, $C_nH_{2n-4}O_4SO_4$, $C_nH_{2n-2}O_5SO_4$, $C_nH_{2n-4}O_5SO_4$, and $C_nH_{2n-4}O_6SO_4$, respectively (n>4).

Figure 5. (a–c) CH_2-Kendrick diagrams and (d–e) Van Krevelen diagrams for CHONS. The color-coding indicates the DBE values calculated from Eq 1. The molecular formulas of the homologue series 1 to 10 can be written as $C_nH_{2n+1}NO_3SO_4$, $C_nH_{2n-1}NO_3SO_4$, $C_nH_{2n+1}ONO_3SO_4$, $C_nH_{2n-1}ONO_3SO_4$, $C_nH_{2n-1}O_2NO_3SO_4$, $C_nH_{2n-5}ONO_3SO_4$, $C_nH_{2n-3}O_2NO_3SO_4$, $C_nH_{2n-1}O_3NO_3SO_4$, $C_nH_{2n-3}O_3NO_3SO_4$, and $C_nH_{2n-3}O_4NO_3SO_4$, respectively (n>4).

Figure 6. Number of C atoms of CHOS and CHONS as a function of molecular weight in the Shanghai samples. Note that only compounds with a relative abundance greater than or equal to 0.5% of that of $C_{10}H_{17}O_7N_1S_1$ in the SHSN sample are shown in this figure.
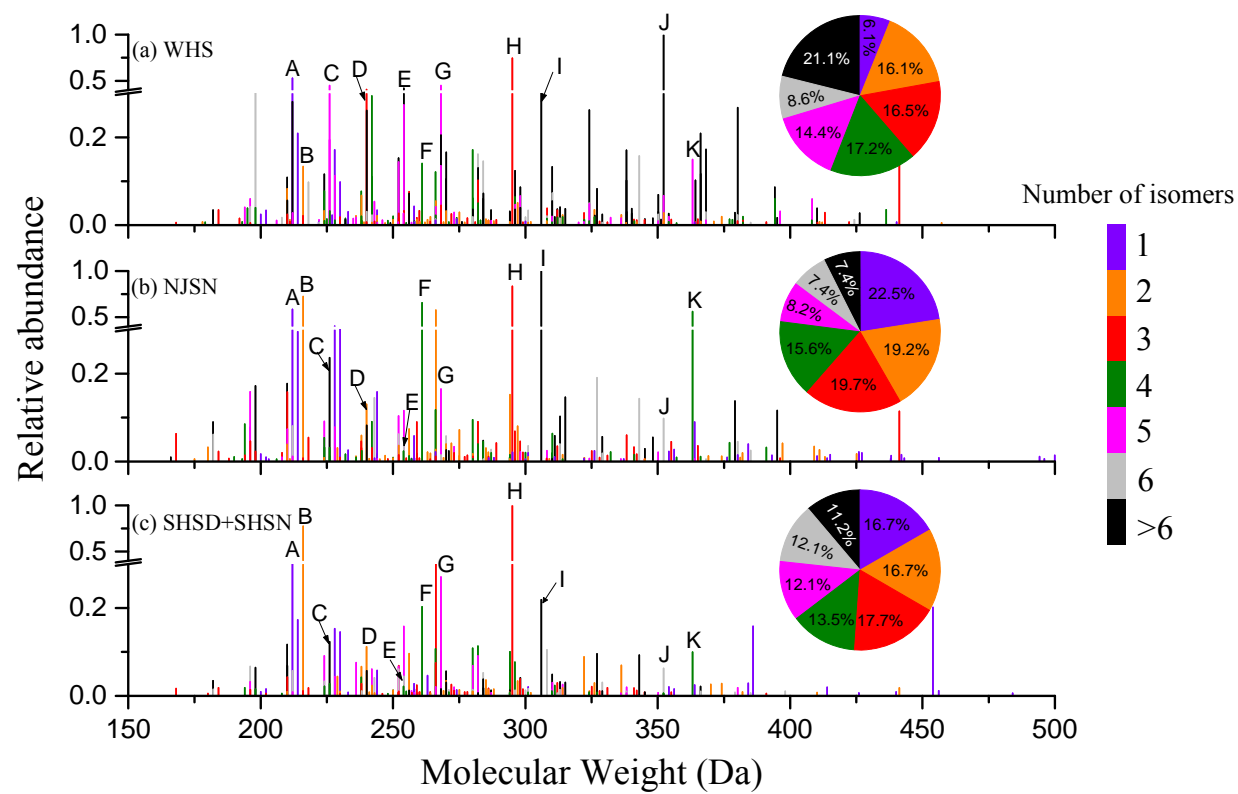
Figure 7. Relative abundance distributions of CHOS and CHONS in the Shanghai samples. Note that only compounds with a relative abundance greater than or equal to 0.5% of that of $C_{10}H_{17}O_7N_1S_1$ in the SHSN sample are shown in this figure.
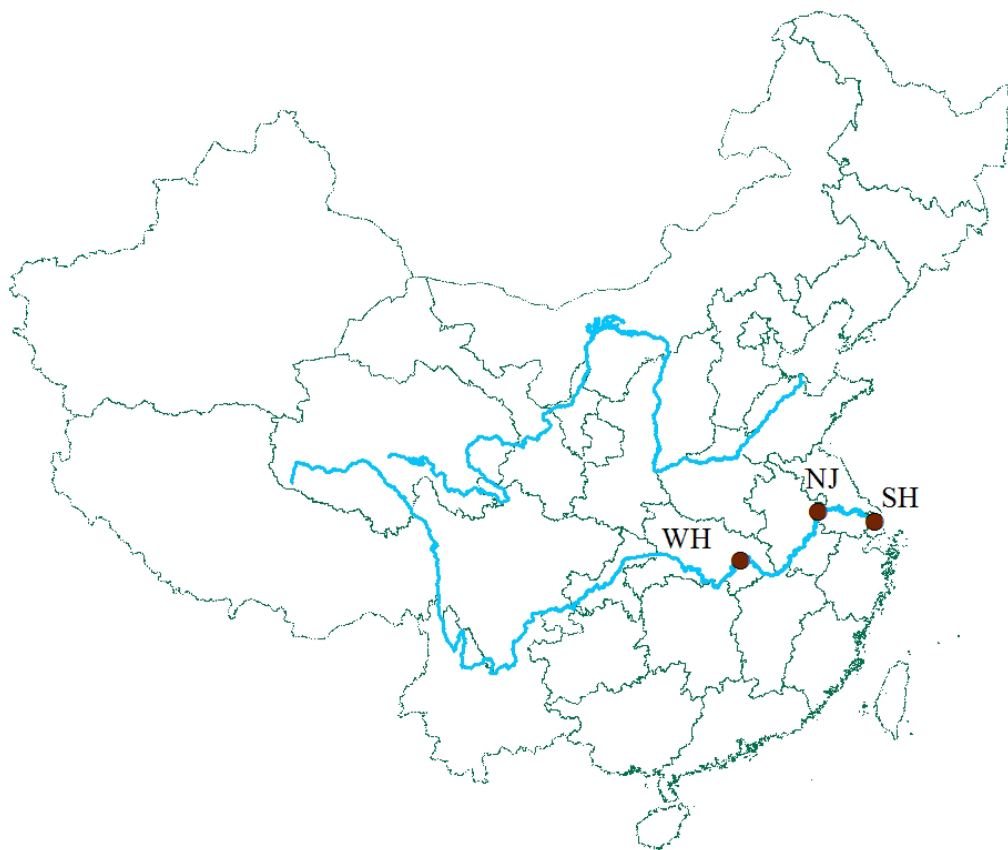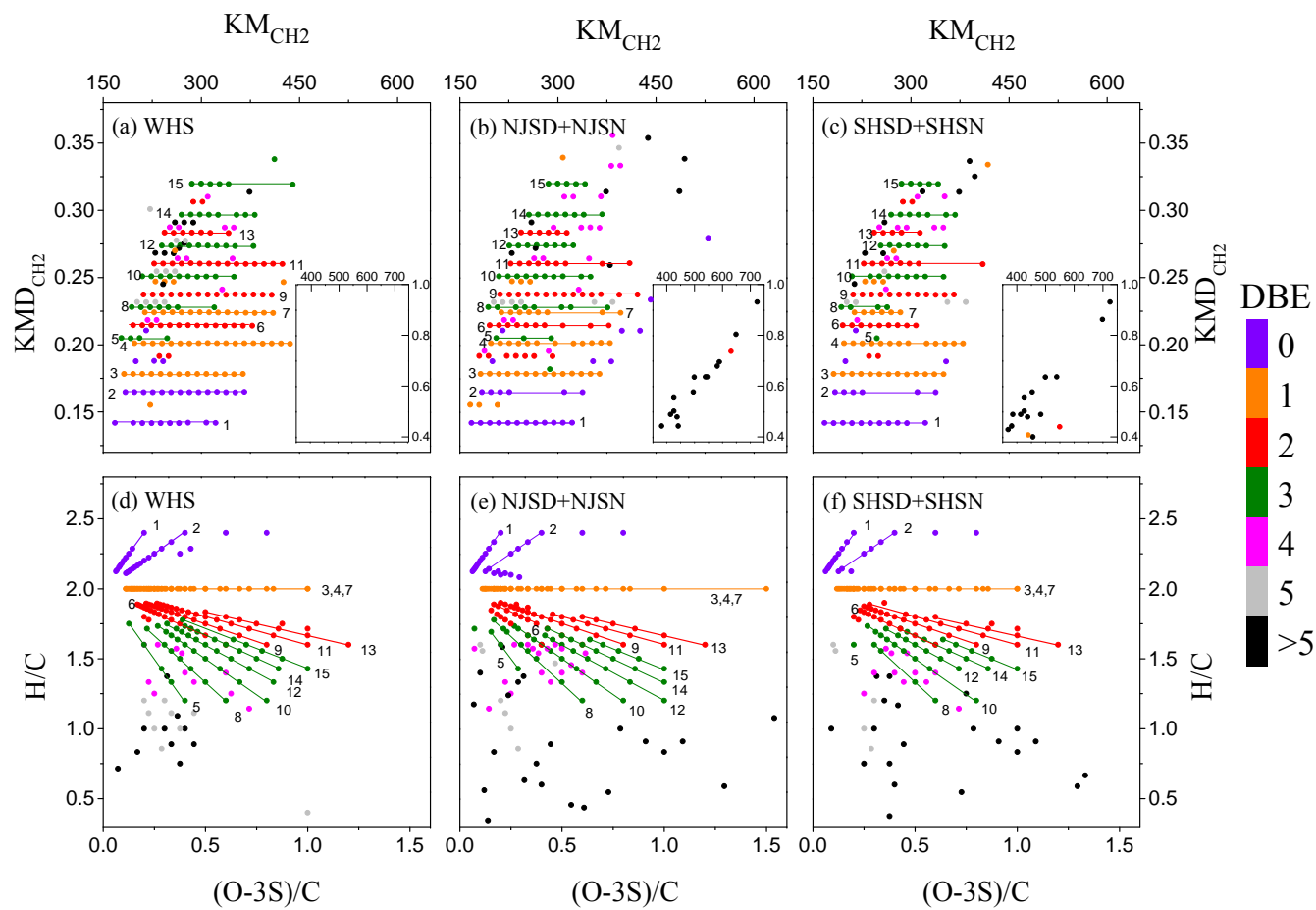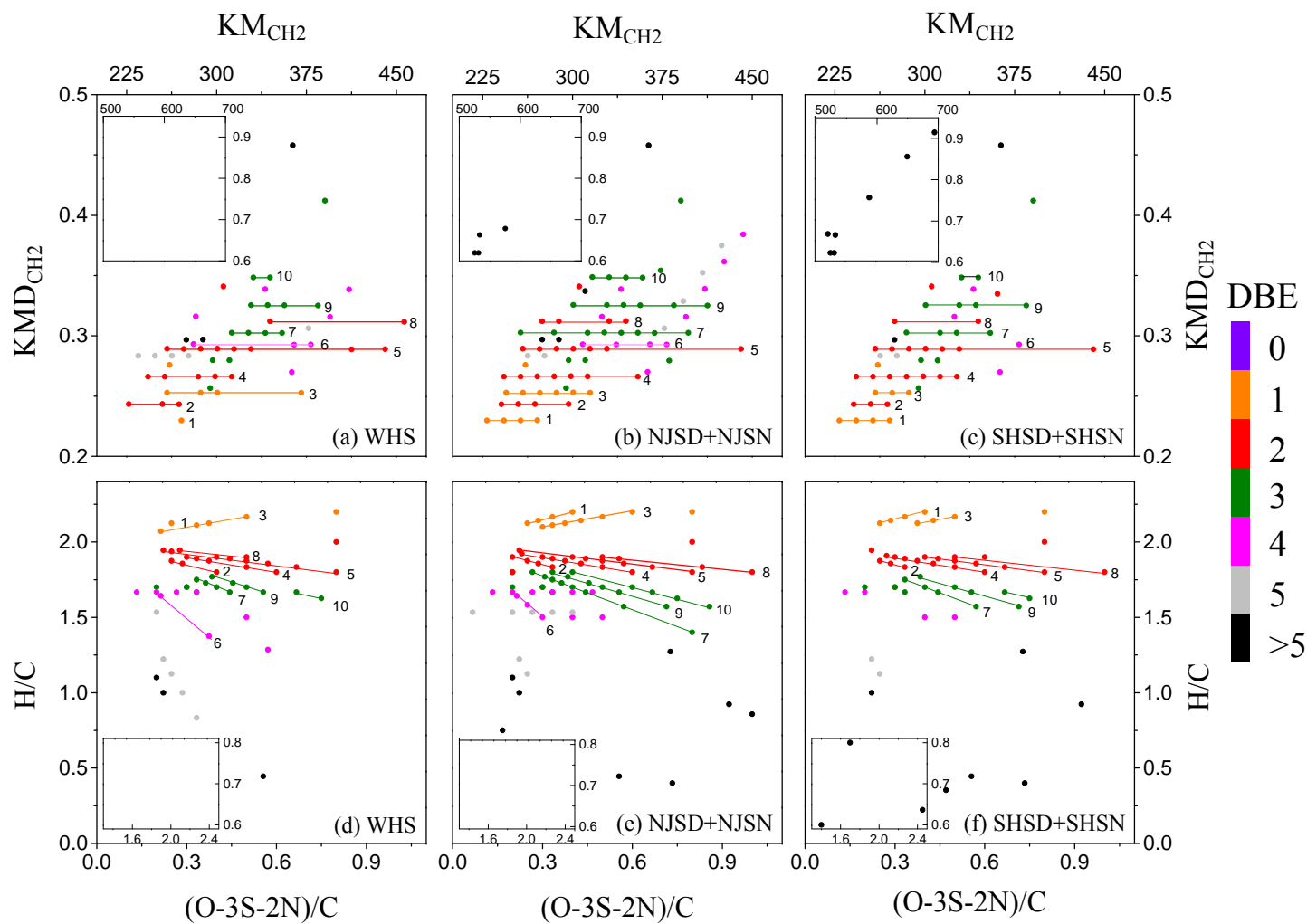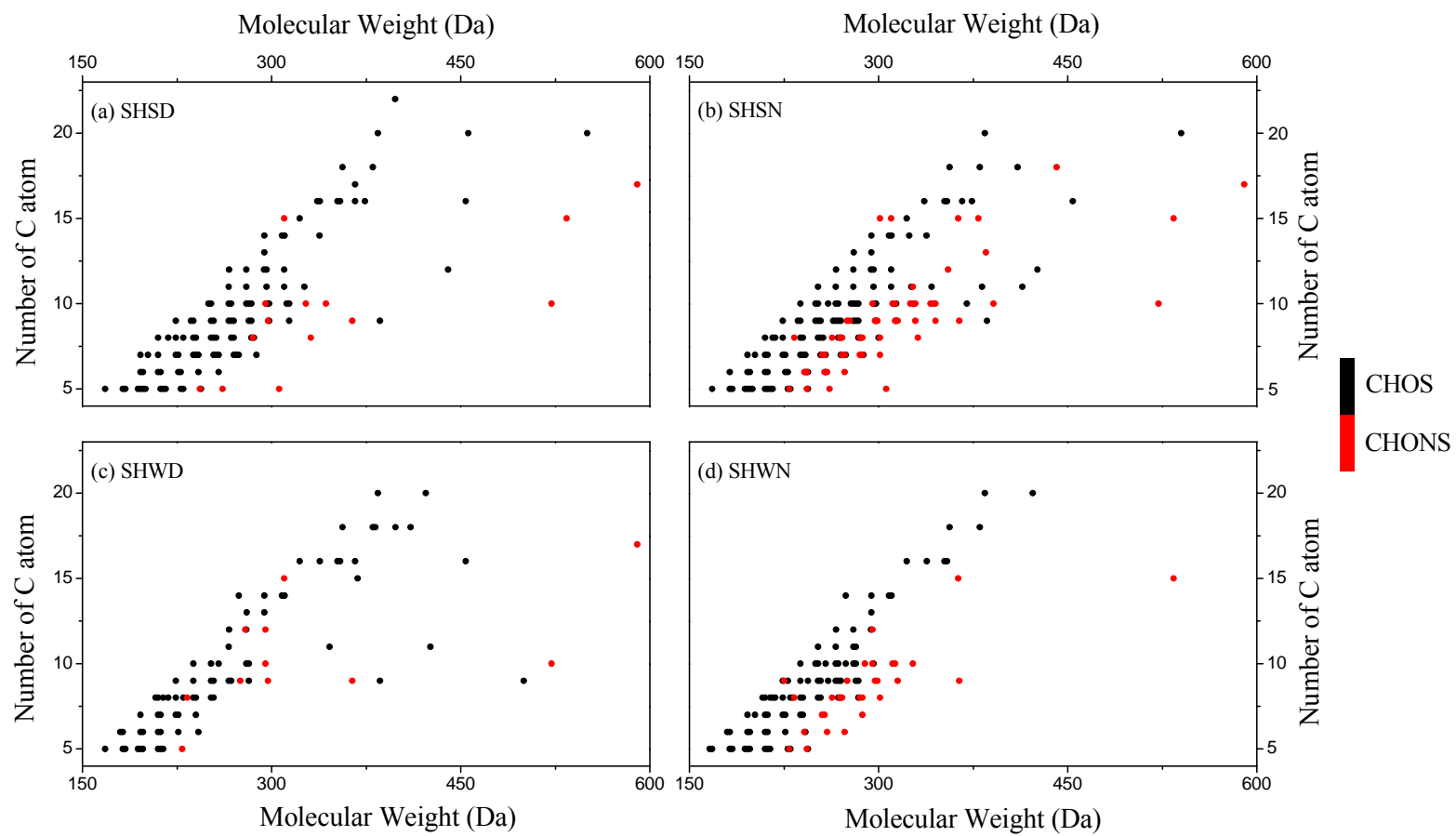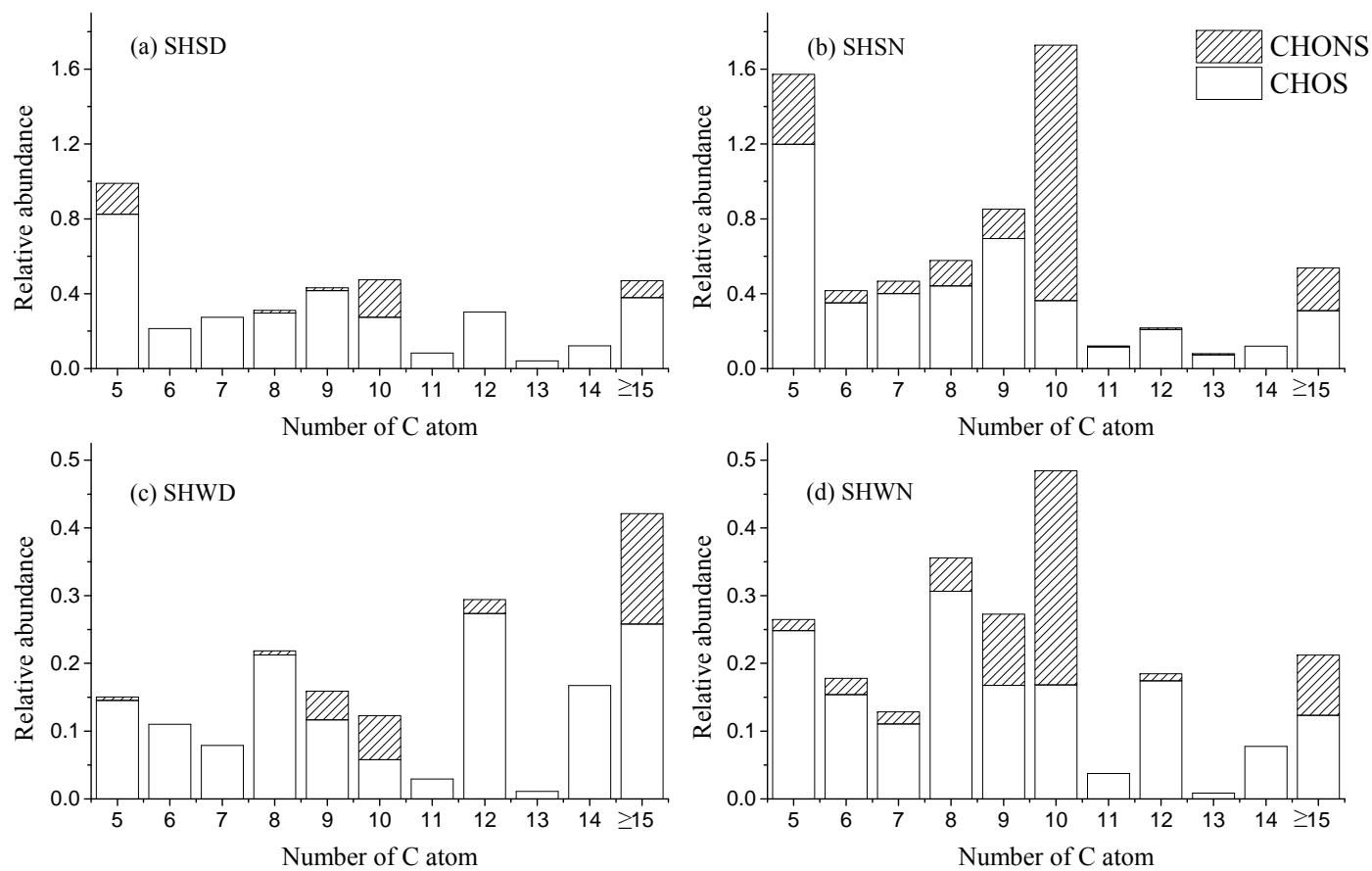
Figure 1
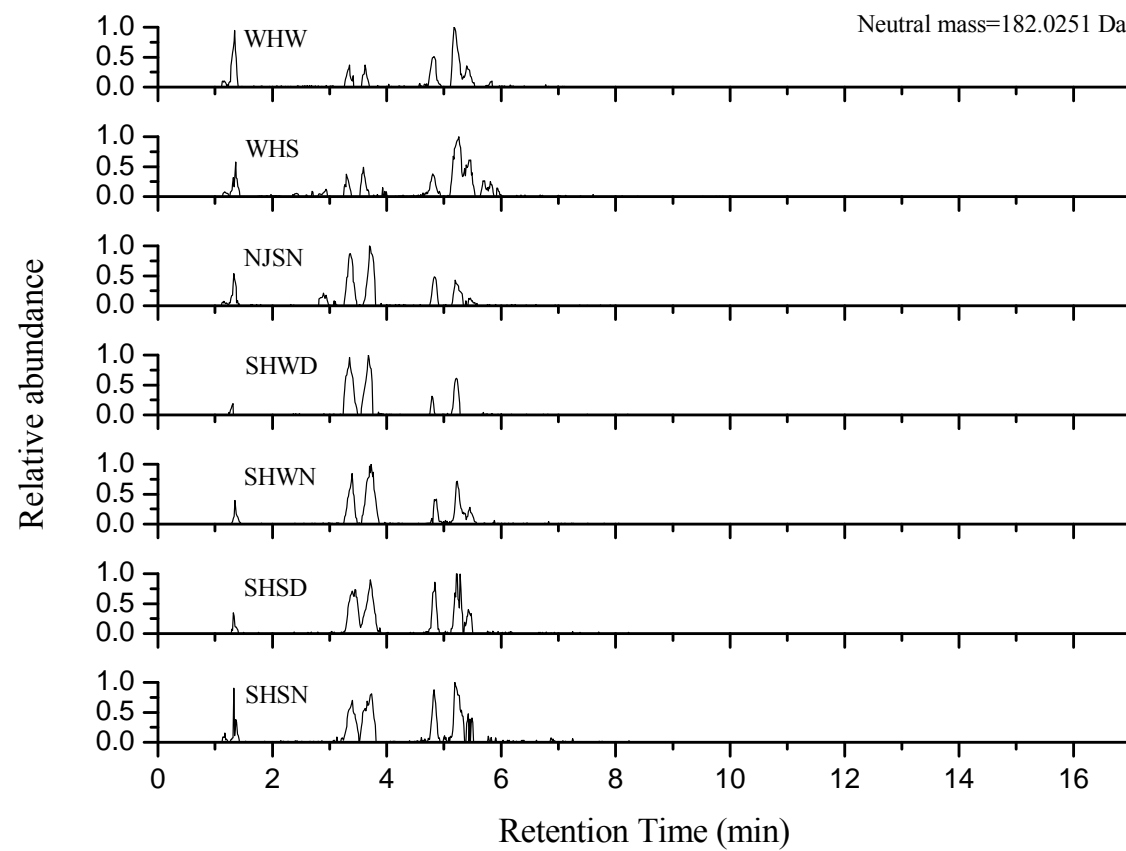
Figure 2

Figure 3

Figure 4

Figure 5

Figure 6

Figure 7